

On the Clustering Properties of Mini-Jet and Mini-Dijet in High-Energy pp Collisions

Cheuk-Yin Wong¹, Liwen Wen², Gang Wang², Huan Zhong Huang^{2,3}

¹*Physics Division, Oak Ridge National Laboratory,
Oak Ridge, TN 37831, USA*

²*Department of Physics and Astronomy,
University of California, Los Angeles, California 90095, USA*

³*Key Laboratory of Nuclear Physics and Ion-beam Application (MOE) and Institute of Modern Physics,
Fudan University, Shanghai 200433, China*

(Dated: July 13, 2021)

Mini-jets and mini-dijets provide useful information on multiple parton interactions in the low transverse-momentum (low- p_T) region. As a first step to identify mini-jets and mini-dijets, we study the clustering properties of produced particles in the pseudorapidity and azimuthal angle space, in high-energy pp collisions. We develop an algorithm to find mini-jet-like clusters by using the k-means clustering method, in conjunction with a k-number (cluster number) selection principle. We test the clustering algorithm using minimum-bias events generated by PYTHIA8.1, for pp collision at $\sqrt{s} = 200$ GeV. We find that multiple mini-jet-like and mini-dijet-like clusters of low- p_T hadrons occur in high multiplicity events. However similar clustering properties are also present for particles produced randomly in a finite pseudorapidity and azimuthal angle space. The ability to identify an azimuthally back-to-back correlated mini-jet-like clusters as physical mini-jets and mini-dijets will therefore depend on the additional independent assessment of the dominance of the parton-parton hard-scattering process in the low- p_T region.

PACS numbers: 13.85.Hd, 13.75.Cs

I. INTRODUCTION

The mechanism of relativistic parton-parton hard-scattering is an important basic perturbative QCD process in particle production in high-energy nucleon-nucleon collisions [1–29]. Because of the composite nature of a nucleon, multiple hard-scattering between projectile nucleon partons and target nucleon partons will lead to the production of jets and dijets whose subsequent fragmentation gives rise to the production of particle clusters. It is distinctly different from the nonperturbative flux-tube fragmentation process [6, 10, 25, 30–46] in which a quark of one nucleon and the diquark of the other nucleon (or a gluon of one nucleon and the gluon of the other nucleon [47–52]) form one flux tube and the subsequent fragmentation of the flux tube leads to the production of hadrons. It is also different from the direct-fragmentation process [53] in which the partons from the composite nucleon fragment directly into the detected particles.

The hard-scattering process was originally proposed as the dominant process for the production of high- p_T jet clusters, of order many tens of GeV/c [1–7]. However, the UA1 Collaboration found that it is also the dominant process for the production of particle clusters with a total p_T of a few GeV/c, for $p\bar{p}$ collisions at $\sqrt{s}=0.2$ to 0.9 TeV [15]. The term “mini-jet” was introduced to describe low- p_T jet clusters [16]. The dominance of jet production can be extended to lower and lower p_T domains at high collision energies because (i) the fraction of particles produced by such a process increases rapidly with collision energies \sqrt{s} , and (ii) the jet-production invariant cross section at mid-rapidity varies as an inverse power of p_T [8, 16, 17, 27, 29, 54].

Recently, the region of dominance of the hard-scattering process has been found to extend to the production of hadrons in the even lower p_T region of a few tenths of a GeV/c [26–29]. An indirect piece of evidence comes from the observation on the transverse momentum spectra of produced hadrons: For the production of particles with p_T within the range from a few tenths of a GeV to a few hundred GeV in high-energy pp and $p\bar{p}$ collisions at $\sqrt{s}=0.9$ to 7 TeV, the hadron transverse spectra, whose magnitude spans over 14 decades of magnitude, can be described by a simple Tsallis inverse-power-law type distribution with only three degrees of freedom [26–29]. The simplicity of the power-law type transverse spectra suggests that only a single mechanism, the hard-scattering process, dominates over the extended p_T domain. An additional piece of direct evidence comes from the jet-like structure in the two-hadron angular ($\Delta\eta, \Delta\phi$) correlation data in a minimum- p_T -bias measurement of the STAR Collaboration in pp collisions at $\sqrt{s} = 200$ GeV [55–58]. The two-particle angular correlations of these low- p_T particles exhibit the signature of parton-parton scattering. Furthermore, the momentum distributions of hadrons associated with a hadron trigger of a few GeV/c in pp collisions at $\sqrt{s} = 200$ GeV exhibit a jet-like cluster structure within a cone, as observed by the STAR Collaboration [59–66] and the PHENIX Collaboration [66, 67].

The extension of the dominance of the hard-scattering model to the low- p_T domain of a few tenths of GeV/c raises serious questions on the large and divergent pQCD corrections at low p_T and the competition from the nonperturbative flux tube fragmentation process associated with low- p_T phenomena. We need additional theoretical and experimental comparisons of the hard-scattering model to construct the proper phenomenological descrip-

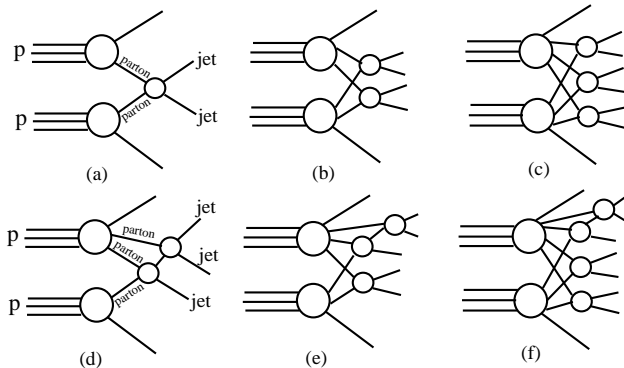


FIG. 1. Various multiple collision diagrams in a pp hard-scattering leading to the production of jets, which are called mini-jets when the transverse momentum of the jet is small. Shown here are diagrams for the production of (a) a dijet pair, (b) two dijet pairs, and (c) three dijet pairs. Furthermore, a scattered parton can make an additional collision with a different parton of the other proton, as shown in diagrams (d), (e), and (f).

tion in the low- p_T region.

If the hard-scattering process of the pp collision is appropriate also for the low- p_T region, then multiple parton interactions (MPI, known also as multiple collision processes) [1, 7, 11–14] must occur to produce multiple mini-jets and mini-dijets [1, 7, 8, 11–17]. Among many other diagrams, the hard-scattering process can lead to the production of one, two, three pairs of mini-dijets as depicted in Figs. 1a, 1b, and 1c. Furthermore, a parton of one proton can make multiple collisions (known also as re-scattering [14]) with different partons of the other proton, as depicted in Figs. 1d, 1e, and 1f. The numbers of produced mini-jets can be even, as in Figs. 1a, 1b, and 1c, or odd, as in Figs. 1d, 1e, and 1f. There can also be additional higher-order diagrams with the radiation and the absorption of gluon partons, which lead to additional mini-jets.

For the production of high- p_T jets, the multiple parton scattering processes have been observed in high energy pp or $p\bar{p}$ collisions [68–71]. Theoretical discussions on the production of mini-jets beyond the leading order has also been investigated, and hard inclusive dijet production with multiparton interactions has also been considered [18–24, 27, 72]. However, in the low- p_T region, the experimental evidence for multiple parton interactions with the production of multiple mini-jets and mini-dijets remains lacking.

We would like to develop tools to study multiple hard-scattering processes, for the production of multiple mini-jets and mini-dijets in the low- p_T domain in pp collisions at high energies. As a first step, we examine here the clustering properties of mini-jets in the pseudorapidity and azimuthal angle space and search for an algorithm

for finding mini-jet clusters.

The production processes for low- p_T particles are not only of intrinsic importance with regard to the underlying mechanism for low- p_T particle production, they are also of extrinsic application values because the nucleon-nucleon collision lies at the heart of a nucleus-nucleus collision, and the low- p_T particle production dominates the particle production process. An understanding of the mechanism of low- p_T particle production in nucleon-nucleon collisions provide vital information on the initial conditions that may exist at the early stage of nucleus-nucleus collisions, for which much interest has been focused recently.

With the observation of the near-side ridge in high-multiplicity events in high-energy pp collisions [59–66, 73–80], the initial dynamics of the system after the production of a jet or a mini-jet [80] depends on the initial configuration of the system. The examination of such a system also calls for an event-by-event study of the multiple mini-jet and mini-dijet productions in pp collisions.

Our event-by-event study has been stimulated by a similar investigation for particle production at lower pp collision energies where the particle production process may be dominated by flux-tube fragmentation [81]. There, the basic conservation laws and the semi-classical picture of the fragmentation process provide powerful tools to reconstruct the space-time dynamics of the pair production processes that may occur, if exclusive data for the production process can become available. In the present investigation, the space-time dynamics of parton-parton hard-scatterings may provide useful experimental information on the multiple collision processes and on the constituent nature of the colliding nucleons.

This paper is organized as follows. In Section II, we summarize the properties of a mini-jet from previous studies. In Section III, we introduce the algorithm for finding mini-jet-like clusters in the pseudorapidity and azimuthal angle space. The algorithm consists of the k-means clustering method and the k-number (cluster number) selection principle, based on the physical properties of mini-jet clusters. We illustrate the usage of such an algorithm in Section IV, using sample events with high multiplicities generated by PYTHIA8.1. We examine the change of the clustering behavior as a function of increasing multiplicities in PYTHIA8.1 events in Section V. We investigate whether similar properties of clustering can be found in a random distribution within the same finite (η, ϕ) phase space in Section VI. We present our conclusions and discussions in Section VII. We discuss another method of finding the cluster number, the elbow method, and note its ambiguities in the Appendix.

II. PROPERTIES OF A MINI-JET

Information on the signatures and the structure of a mini-jet in the (η, ϕ) scatter plot can be inferred from the distribution of the two-hadron angular correlation as

a function of the pseudorapidity difference $\Delta\eta = \eta_2 - \eta_1$ and the azimuthal angular differences $\Delta\phi = \phi_2 - \phi_1$ of the two particles detected with angular coordinates (η_1, ϕ_1) and (η_2, ϕ_2) in coincidence [55–67]. The mini-jet structure appears as a cluster of particles in the (η, ϕ) space (and a cone in three-dimensional configuration space) as indicated by a two-hadron Gaussian distribution in $\Delta\eta$ and $\Delta\phi$ in the form

$$\frac{dN}{d\Delta\eta d\Delta\phi}(\Delta\eta, \Delta\phi) \propto \exp \left\{ -\frac{(\Delta\eta)^2 + (\Delta\phi)^2}{2\sigma_\phi^2} \right\}, \quad (1)$$

where the quantity σ_ϕ was found to be [66]

$$\sigma_\phi = \frac{\sigma_{\phi 0} m_a}{\sqrt{m_a^2 + p_{T, \text{trigger}}^2}}, \quad \sigma_{\phi 0} = 0.5, \quad m_a = 1.1 \text{ GeV}, \quad (2)$$

when triggered by a hadron with transverse momentum $p_{T, \text{trigger}}$. In the minimum-bias data at RHIC energies we shall consider, the quantity $p_{T, \text{trigger}}$ takes on the average value of $\langle p_T \rangle$, which is of order 0.4 GeV/c, and Eq. (2) therefore yields $\sigma_\phi \simeq 0.5$. The two-particle distribution of Eq. (1) has a half-width at half maximum at $R = \sqrt{(\Delta\eta)^2 + (\Delta\phi)^2} = 1.2\sigma_\phi = 0.6$.

We can consider a circle of radius R in the (η, ϕ) plane. The minimum separation between any two points inside the circle is zero and the maximum separation is $2R$. Setting $2R = 2.4\sigma_\phi$ (or $R = 0.6$) will allow the circle to contain a large fraction (about 95%) of the Gaussian distribution (1) within the circular domain. One of the signatures of a mini-jet cluster of particles can be indicated by a cluster of particles within a radius of $R \simeq 0.6$ in the plane of (η, ϕ) .

In the hard-scattering process in the collision of two partons, $a + b \rightarrow a' + b'$, the partons a' and b' materialize subsequently as mini-jets. The initial a and b partons may be endowed with an intrinsic transverse momentum k_T of the order of 0.6 to 1.0 GeV/c [3, 82–84]. To detect final partons a' and b' in the central rapidity region, the conservation of 4-momentum requires that the initial longitudinal momenta of the colliding partons will be converted essentially into the magnitudes of the transverse momenta and the scattered partons a' and b' will come out azimuthally in nearly back-to-back directions. For the scattering of low- p_T partons whose longitudinal momenta are comparable to their intrinsic transverse momenta as we envisage here, we expect approximate back-to-back correlation with considerable fluctuations. The signature of a mini-dijet can be taken to be a pair of min-jets whose azimuthal angles are approximately correlated within the range of $\pi - R$ to $\pi + R$.

III. ALGORITHM FOR FINDING MINI-JET-LIKE CLUSTERS

As discussed in the last section, a mini-jet shows up as a cluster of particles with a cone radius of $R = 0.6$ in

the (η, ϕ) space. Such a cluster can be searched by the k-means clustering method [85–91], in conjunction with an additional k-number (cluster-number) specification principle. In such a search, we ascribe the characteristic mini-jet radius $R = 0.6$ to a cluster and we name it a “mini-jet-like” cluster. In practical terms, two mini-jet-like clusters that are azimuthally correlated in a back-to-back manner may be identified as a physical mini-dijet of two correlated mini-jets at high collision energies, if the mini-jet producing hard-scattering process has been confirmed to be dominant in the low- p_T region as suggested in earlier studies [26, 29, 55–58].

For a given set of M produced particles specified by their angular positions, $\{\mathbf{x}_i = (\eta_i, \phi_i), i = 1, 2, 3, \dots, M\}$, and a given K number of clusters, the k-means clustering method consists of (i) partitioning the set of M particles into K cluster subsets, $S_k = \{\mathbf{x}_i^k\}$, $k = 1, 2, \dots, K$, and (ii) finding for each cluster subset the corresponding cluster center $\{\mathbf{C}_k, k = 1, 2, \dots, K\}$ so as to minimize the potential function

$$\Phi(K) = \sum_{k=1}^K \left\{ \sum_{\mathbf{x}_i^k \in S_k} (\mathbf{x}_i^k - \mathbf{C}_k)^2 \right\}, \quad (3)$$

which is defined as the total subset sum of the squares of the distances between the cluster subset points and their corresponding cluster center \mathbf{C}_k .

For a fixed value of K , the variation of the above potential function $\Phi(K)$ with respect to the cluster center \mathbf{C}_k is given by

$$\delta\Phi(K) = - \sum_{k=1}^K \left\{ \sum_{\mathbf{x}_i^k \in S_k} 2(\mathbf{x}_i^k - \mathbf{C}_k) \cdot \delta\mathbf{C}_k \right\}. \quad (4)$$

Because all $\delta\mathbf{C}_k$ are independent, the minimization of $\Phi(K)$ with respect to the variation of the positions of the cluster centers \mathbf{C}_k leads to $\delta\Phi(K)/\delta\mathbf{C}_k = 0$ and

$$\sum_{\mathbf{x}_i^k \in S_k} 2(\mathbf{x}_i^k - \mathbf{C}_k) = 0. \quad (5)$$

This yields \mathbf{C}_k as the centers of gravity of the subset of points of $S_k = \{\mathbf{x}_i^k\}, k = 1, 2, \dots, K$,

$$\mathbf{C}_k = \frac{1}{M_k} \sum_{\mathbf{x}_i^k \in S_k} \mathbf{x}_i^k, \quad (6)$$

where $M_k = (\sum_{\mathbf{x}_i^k \in S_k} 1)$ is the number (multiplicity) of particles in the subset S_k .

In numerical implementation of the k-means clustering method, one chooses randomly the first cluster center as one of the data points and chooses randomly the other $K-1$ cluster centers in the other data points with probability proportional to the square of the distance from the first cluster center [89]. For each data point, the knowledge of the positions of the initial cluster centers then

allows one to calculate the squares of the distance between the data point and all K cluster centers. To each data point, one then assigns the data point to the subset S_k with the smallest square of distance to its cluster center \mathbf{C}_k . After all subset assignments to S_k have been completed for all data points, the center of gravity of the data points in each new subset S_k is then re-calculated to give the new cluster centers \mathbf{C}_k , with which the iterative procedure will proceed until it is convergent. One then calculates the potential function $\Phi(K)$ of Eq. (3) as the sum of squared distances.

The above standard procedure is then repeated with other random initialization of the initial cluster centers. After many cluster center random initializations and the corresponding convergent solutions and the potential functions $\Phi(K)$ have been obtained, the proper solution for the case of a given value of K can be found and selected as the solution with the minimum value of the potential function $\Phi(K)$. For a given value of K , the k-means clustering method then yields uniquely the cluster subsets of particles $S_k = \{\mathbf{x}_i^k\}$, $k = 1, 2, \dots, K$ associated with each cluster and the corresponding cluster center location \mathbf{C}_k .

The k-means clustering method needs an amendment to make it applicable for mini-jet-like cluster searches because the method will lead to poorly displaced and inaccurate cluster centers, if particle points that are obviously not part of a cluster and quite far away from a cluster have been included into the particle data set in the clustering algorithm. The presence of these ‘non-cluster’ particles are possible because there may be other sources of particle production in addition to those from clusters within the narrow window of acceptance. We need to use our knowledge on the structure of the mini-jet in Eq. (1) to sieve out these non-cluster data points in the set of M particles. We calculate the distances between any data point and all other data points in the (η, ϕ) plane. The knowledge of these distances allows us to exclude any data point whose minimum separation to all other data points exceeds a distance $2R$, presumably the maximum separation for two data points in a mini-jet. After these points are excluded to yield a reduced set of particles belonging to clusters in this modification, the k-means clustering method becomes very efficient, fast-converging, and capable of yielding accurate cluster centers. The method is stable against the variations of the positions of the cluster centers which turn out to be the centers of gravity of the subset S_k of the clustering points, as given by Eq. (6). In this procedure, because the azimuthal angle ϕ is equivalent to $\phi \pm 2\pi$ with a modulo of 2π , it is important to wrap around the azimuthal angles when such a wrapping leads to additional possibility of mini-jet clustering.

The k-means clustering method requires a prior knowledge of the cluster number K . There may be different ways to partition a group of M particles into different numbers of clusters and the locations of the cluster centers may also vary. The selection of K and the identifica-

tion of particles as belonging to different K clusters may therefore be ambiguous. Our algorithm to find mini-jet-like clusters must contain an additional method to select the appropriate cluster number K that is based on well-founded physical principles.

For a given set of M produced particles on the (η, ϕ) plane, one considers a possible range of cluster K numbers, $K = K_{\min}, \dots, K_{\max}$. The maximum limit K_{\max} occurs when the cluster number $K_{\max}+1$ leads to the dis-allowed case of having a cluster with only a single particle. For each cluster number K in the range under consideration, the k-means clustering method leads to a unique partition into K clusters with their corresponding cluster centers \mathbf{C}_k . To select the appropriate K , we use the mini-jet physical properties discussed in the last section that a cluster circle with a radius $R=0.6$ of a physical mini-jet contains almost all of the particles of the physical mini-jet. In order for the cluster number K to lead to the appropriate partition of the set of M particles into K physical mini-jet or mini-jet-like clusters, the corresponding K cluster circles with a radius $R = 0.6$ should contain all, or almost all, M data points of the set. There should be very few data points outside the cluster circles. The k-number (cluster number) selection principle is therefore that *K should be the cluster number that leads to the fewest number of data points outside the cluster circles with a radius $R=0.6$* . If there are two K values having the same fewest outside points, we should select the smaller K value because the set of the smaller number of mini-jets can radiate a parton and become the parent of the set with a greater number of mini-jets.

Our mini-jet-like cluster finding algorithm therefore consists of the k-means cluster method, supplemented by the k-number selection principle of the fewest number of data points outside of the cluster circles.

IV. ILLUSTRATION OF THE ALGORITHM FOR FINDING MINI-JET-LIKE CLUSTERS

We shall apply the above algorithm for finding mini-jet-like clusters from charged hadrons generated by the PYTHIA8.1 for high-energy pp collisions at $\sqrt{s}=200$ GeV. The event generators PYTHIA8.1 [9] and PYTHIA6.4 [8] include the multiple parton interaction processes as described in Ref. [7], with additional considerations on color correlations, flavour correlations, junction topology, beam remnant configurations [11], and interleaving initial state radiations [12]. The fully interleaving evolution [13] and re-scattering [14] are further included in PYTHIA8.2 [10].

In the series of PYTHIA programs, the basic picture of the multiple collision process arises from the composite nature of the proton which possesses a parton spatial density distribution in addition to the standard parton momentum distribution function (parton PDF). The parton-parton collisions between the constituents of the projectile proton and the target proton are assumed to

be independent of each other, and the number of collisions in an event is therefore given by a Poisson distribution. The probability of parton-parton collisions is then a function of the parton-parton cross section and the impact parameter. To extend the parton-parton scattering cross section to the low- p_T region for minimum-bias studies, the divergent parton-parton scattering cross section at low transverse momenta has to be regularized with a cut-off parameter that can be chosen to yield the appropriate charged-hadron multiplicity distribution. We expect finite multiple parton-parton multiple collision probabilities for the independent collisions of projectile partons with target partons, as depicted in the diagrams in Fig. 1. They lead to the production of multiple mini-jets and mini-dijets in the angular scatter plot of produced charged particles.

The probability for the occurrence of multiple mini-jets and mini-dijets depends on the charge multiplicity of the event, which is part of the total hadron multiplicity. For brevity of notation and its frequent usage, we shall abbreviate “charge multiplicity” or “charged-particle multiplicity” simply by “multiplicity”, when ambiguities do not arise or are not pertinent. We shall restore back the term “charge multiplicity” when it is properly needed.

In order to predict what may be expected experimentally for multiple mini-jet and mini-dijet productions, we generate minimum-bias events using the PYTHIA8.1 and we accept primary charged particles with $|\eta| \leq 1$. For each event multiplicity, we select 5 random events for analysis. Each event will be labeled by $pMeI$, where pM stands for PYTHIA minimum-bias event with charge multiplicity M , and eI denotes the I th event with the charge multiplicity M . We would like to search for the presence of the expected mini-jet-like and mini-dijet-like clusters from the angular scatter plots of charged particles in these events.

The detected and identified charged particles include not only charged hadrons but also a small percentage (of about 12%) of e^+ or e^- . By convention, we include these leptons in our charged multiplicity counts. However, because the e^+ and e^- particles arise from many different hadronic and non-hadronic sources, and the relations between these particles and their hadron parents, if they arise from hadronic decays, are non-trivial, we shall exclude them in our mini-jet finding algorithm. Their presence in the scattered (η, ϕ) plot provides a sense of possible hadronic activities in the vicinity of their angular locations.

In Figs. 2, 4, 5, and 6, we shall show sample scatter plots of charged particles in the (η, ϕ) plane from minimum-bias events generated by the PYTHIA8.1 event generator. We display the particle labels of kaons, protons, electrons, and muons while the other particles are all charged pions. The solid and open points denote positive and negative particles respectively, and circular and square points denote $p_T \geq 0.5$ GeV/c and $p_T < 0.5$ GeV/c, respectively.

We shall illustrate the algorithm for finding mini-jet-

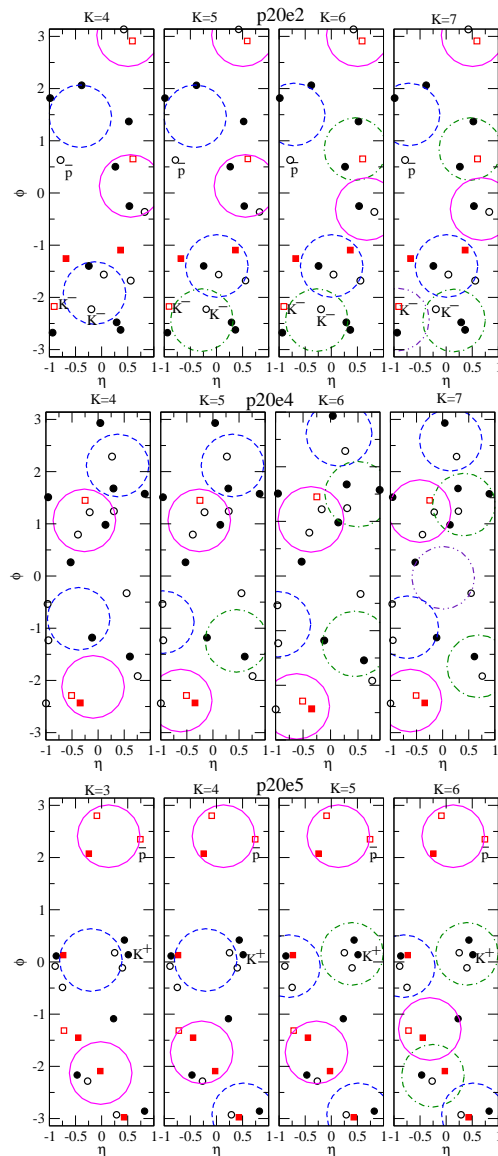


FIG. 2. (Color Online) Scatter plots in the (η, ϕ) plane for produced charged particles in minimum-bias events with multiplicities $M=20$ for $-1 \leq \eta \leq 1$, in sample events p20e2, p20e4, and p20e5, generated by PYTHIA8.1 for pp collisions at $\sqrt{s}=200$ GeV. Cluster circles with a radius $R = 0.6$ circumscribe cluster centers obtained with the k-means clustering method assuming different cluster numbers K .

like clusters with concrete examples. We consider three randomly selected minimum-bias PYTHIA8.1 events with $M=20$ in Fig. 2. For each of these events, we assume different cluster numbers K and, obtain K clusters and their corresponding cluster centers C_k using the k-means clustering method. We then construct cluster circles with a radius $R = 0.6$ circumscribing the cluster centers.

In Fig. 2 for event p20e2, for the cases of $K = 4, 5, 6$, and 7, the number of points outside of the cluster circles are 10, 6, 4, and 2 respectively. For the case of $K=8$, there is no k-means clustering solution without one of

the clusters possessing only a single particle. $K=8$ is therefore excluded from our consideration for this p20e2 event because we do not consider a single particle to be a cluster. If the clusters are mini-jet clusters, then almost all particle points should be inside the cluster circles. The case of $K = 7$ leads to the fewest number of particles outside of the cluster circles. According to the principle of fewest outside points, $K = 7$ is the proper number of clusters for event p20e2. Similarly, for the event p20e4 in Fig. 2 and $K = 4, 5, 6$, and 7 , the number of points outside of the cluster circles are 8, 5, 3, and 0 respectively. We infer that $K = 7$ leads to mini-jet-like clusters. For the event p20e5 and $K=3, 4, 5$, and 6 , the number of outside points are 11, 6, 1 and 0. We infer that $K = 6$ is the proper cluster number with zero points outside of the cluster circles.

It should be mentioned that there is another method, the “elbow method”, to select the cluster number K by studying the K -dependence of the potential function $\Phi(K)$ [85, 90]. The method consists of determining the cluster number by the location of the “kink” where there is a sudden change of the slope of the potential function. The method suffers from the ambiguities in finding where the “kink” lies, and will not be used in the present context. We shall discuss the ambiguities in such a method in Appendix A.

V. SCATTER PLOTS OF PRODUCED CHARGED PARTICLES FROM PYTHIA8.1

We shall study the clustering properties of charged particles produced in pp collisions in minimum-bias events with $-1 \leq \eta \leq 1$, generated by PYTHIA8.1 at $\sqrt{s} = 200$ GeV. In reviewing the scatter plots of these particles in the (η, ϕ) space as a function of the charged particle multiplicity, it should be kept in mind that those events with larger charge multiplicity numbers M are events with lower occurrence frequencies. The multiplicity distribution for this set of particles generated by PYTHIA8.1 is given in Fig. 3. The average number of charged particles within the window of $|\eta| \leq 1$ is $\langle M \rangle = 6.94$.

We plot in Fig. 4 to 6 mini-jet-like clusters of particles within a radius of $R = 0.6$ obtained from the clustering algorithm of finding mini-jet-like clusters. As the multiplicity increases beyond $M=6$, there appears to be a gradual onset of the production of multiple mini-jet-like clusters, using minimum-bias events generated by PYTHIA8.1, for pp collision at $\sqrt{s} = 200$ GeV. Therefore, the search for the non-mini-jet production mechanism will need to focus on events with multiplicity M less than about 6. To examine whether the non-mini-jet mechanism is the flux tube fragmentation, we need more information of identified particles along a greater region of the rapidity space as suggested in [81].

An interesting question arises whether the angular clustering of data points at $(\Delta\eta, \Delta\phi) \sim 0$ may arise from the decay of resonances. As the invariant mass of two

relativistic hadrons with $(\Delta\eta, \Delta\phi) \sim 0$ is nearly zero, the clustering of hadrons around $(\Delta\eta, \Delta\phi) \sim 0$ may not likely arise from resonance decays.

The partitioning of the set of charged particles into mini-jet-like clusters can be carried out on an event-by-event basis in Figs. 4 to 6 by identifying a mini-jet-like cluster as an assemble of particles, represented by a circle in the (η, ϕ) plane with a radius of $R = 0.6$. We can furthermore identify a mini-dijet-like pair of clusters as two correlated mini-jet-like clusters whose centers are separated azimuthally within the range from $\pi - R$ to $\pi + R$. In Figs. 4-6, we indicate a mini-jet-like cluster and its corresponding associated partner by circles of the same line type and color. At the end edges of $\phi = \pm\pi$, the scatter plot are sometimes wrapped around so as to facilitate the partitioning particles into mini-jet-like clusters, as in events p11e2, p11e4, p11e5,...

The data in Figs. 4 to 6 reveal that as the multiplicity increases, mini-jet-like clusters of more than 2 particles within a radius of $R=0.6$ occur with a greater probability. In most of the events with $M = 7$ to 9 and higher multiplicities, a single mini-jet-like cluster appears often to correlate roughly with an associated mini-jet-like partner in azimuthally nearly back-to-back directions. There may be a fluctuation of the back-to-back correlation due to the intrinsic transverse momentum of the partons. We conclude from these figures that mini-dijet-like clusters commence at $M \sim 7$, with the probability increasing gradually as M increases, and appear nearly consistently for $M \gtrsim 11$, as indicated in Figs. 4 and 5.

We show in Figs. 5 the scatter plots of charged particles in events with high multiplicities, $11 \leq M \leq 15$. As the multiplicity number M increases beyond $M \gtrsim 13$ there is a transition from the production of one pair of mini-dijet-like clusters to the production of two pairs of mini-dijet-like clusters, with each pair of mini-dijet-like cluster approximately azimuthally back-to-back with respect to each other. The transition region is not sharp, as

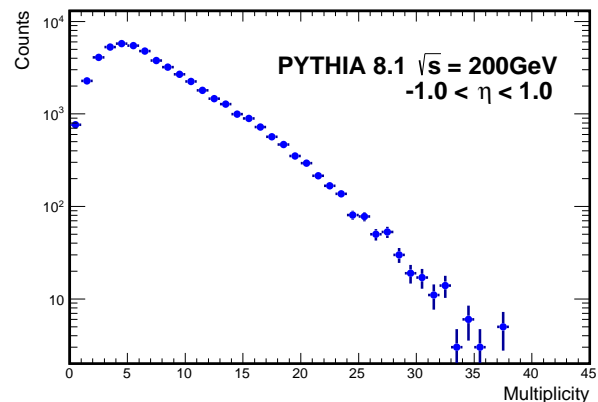


FIG. 3. The multiplicity distribution dN/dM of charged particles within the window $-1 \leq \eta \leq 1$ obtained with PYTHIA8.1, for pp collisions at $\sqrt{s} = 200$ GeV.

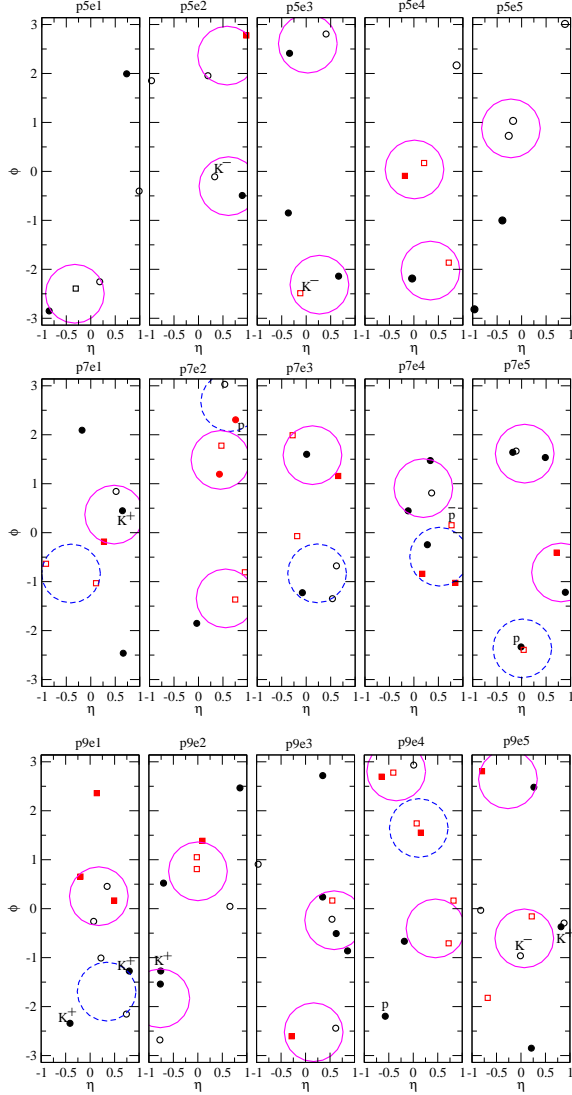


FIG. 4. (Color Online) Scatter plots in the (η, ϕ) plane for produced charged particles in events, with multiplicities $M=5, 7$, and 9 , within $-1 \leq \eta \leq 1$, generated by the PYTHIA8.1 for pp collisions at $\sqrt{s}=200$ GeV. Circular curves indicate the locations of the mini-jet-like clusters.

many events contain only a single pair of mini-dijet-like cluster, while many other events in Fig. 5 contain double correlated mini-dijet-like clusters. We conclude from these figures that two mini-dijet-like cluster pairs begin to set in with $M \gtrsim 14$, with the probability increasing gradually as M increases.

We show in Figs. 6 the scatter plots of charged particles in events with ultra-high multiplicities, $17 \leq M \leq 21$. As the multiplicity number M increases beyond $M \gtrsim 17$, the production of two sets of mini-dijet-like clusters appears nearly consistently, with occasional production of 5 mini-jet-like clusters. In Fig. 6, events with $M \gtrsim 20$ appear to contain events with three pairs of mini-dijet-like clusters.

The results from the present analysis indicates that multiple mini-jet-like clusters and mini-dijet-like clusters

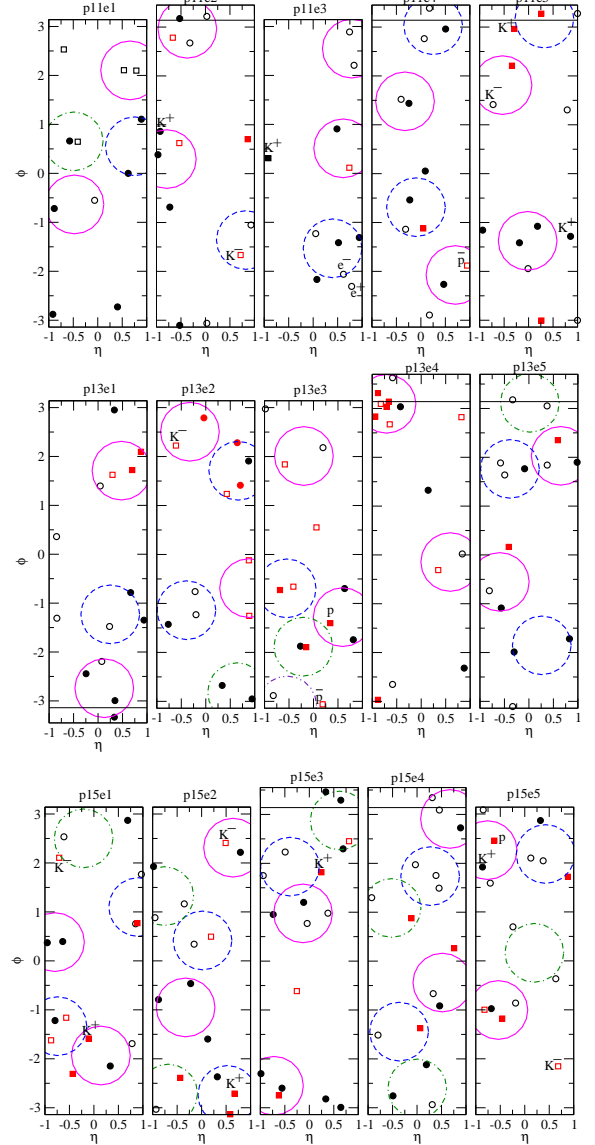


FIG. 5. (Color Online) Scatter plots in the (η, ϕ) plane for $M=11, 13$, and 15 , within the window of $-1 \leq \eta \leq 1$, generated by the PYTHIA8.1 for pp collisions at $\sqrt{s}=200$ GeV. Circular curves indicate the locations of the mini-jet-like clusters.

are common occurrences for events with high multiplicities and their numbers increase with the increasing multiplicity M .

Fig. 7(a) shows that for events generated by PYTHIA8.1 within $p_T \leq 0.15$ GeV/c and $|\eta| \leq 1$, the number of mini-jet-like clusters K appears to be a linear function of charge multiplicity M given by

$$K = (0.268 \pm 0.024)[M + (0.816 \pm 1.272)]. \quad (7)$$

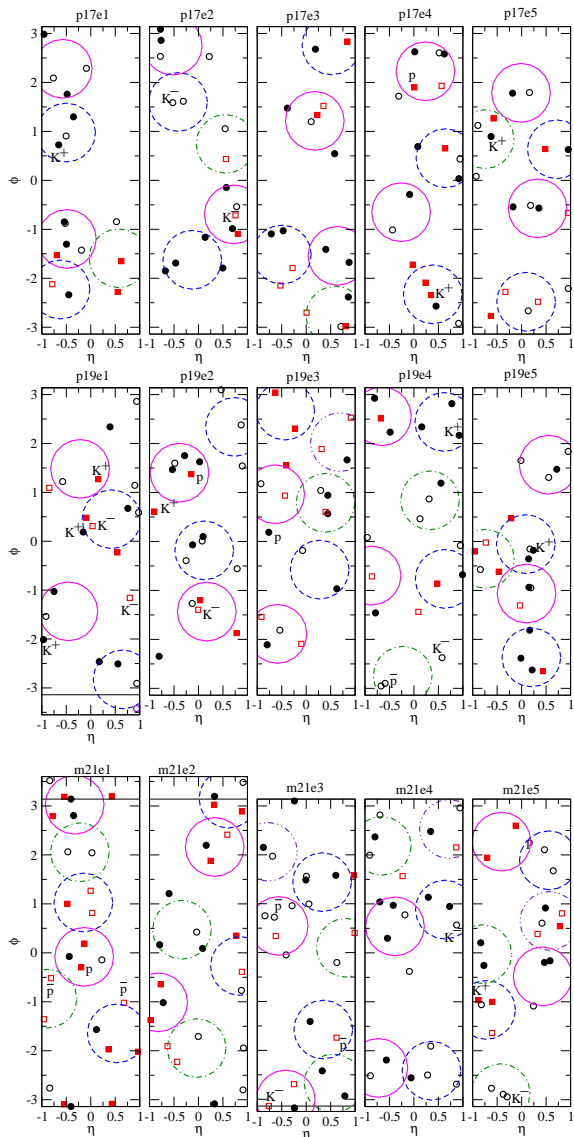


FIG. 6. (Color Online) Scatter plots in the (η, ϕ) plane for $M=17, 19$, and 21 , within the window of $-1 < \eta < 1$, generated by the PYTHIA8.1 for pp collisions at $\sqrt{s}=200$ GeV. Circular curves indicate the locations of the mini-jet-like clusters.

VI. CLUSTERING OF PARTICLES IN A RANDOM DISTRIBUTION WITH UNIFORM PROBABILITIES

The results in the last section indicate the copious production of clusters in the theoretical model of PYTHIA8.1, which contains mainly the mini-jet production mechanism for high-energy pp collisions at $\sqrt{s} = 200$ GeV. Many of these clusters also exhibit back-to-back azimuthal correlations to make them good candidates for physical mini-dijets, and multiple mini-dijets. These theoretical clusters as well as their corresponding experimental counterparts will likely represent physical mini-jets and mini-dijets, if the dominance of the

parton-parton hard scattering process for mini-jet production is extended to the low- p_T region, as suggested by [26, 29, 55–58].

It is worth noting that the clustering property by itself is not sufficient to definitively identify a cluster as mini-jet cluster because similar clustering properties are also present in other particle production models. It is necessary to have other independent collaborative supports for the mini-jet occurrence in order to identify the observed mini-jet-like clusters as likely physical mini-jet clusters.

In order to bring the need for independent collaborative supports into a sharp focus, it is illustrative to examine the clustering properties of particles produced in a simple schematic model in which a total of M' particles are randomly and independently produced with a uniform probability in the (η, ϕ) phase space within the window of $|\eta| \leq \Delta\eta_{\text{window}}/2$ and $|\phi| \leq \pi$,

$$\frac{dP_{\text{random}}}{d\eta d\phi} = \frac{\Theta(\Delta\eta_{\text{window}}/2 - |\eta|) \Theta(\pi - |\phi|)}{2\pi\Delta\eta_{\text{window}}}. \quad (8)$$

This can be the approximate mode of production when particles are produced independently with a uniform probability in rapidity, as from the fragmentation of a flux tube at very high energies [6, 10, 25, 30–46]. It can also be the probability distribution used to describe noise particles randomly produced within the experimental (η, ϕ) phase space. We use different symbols $\{M, K\}$

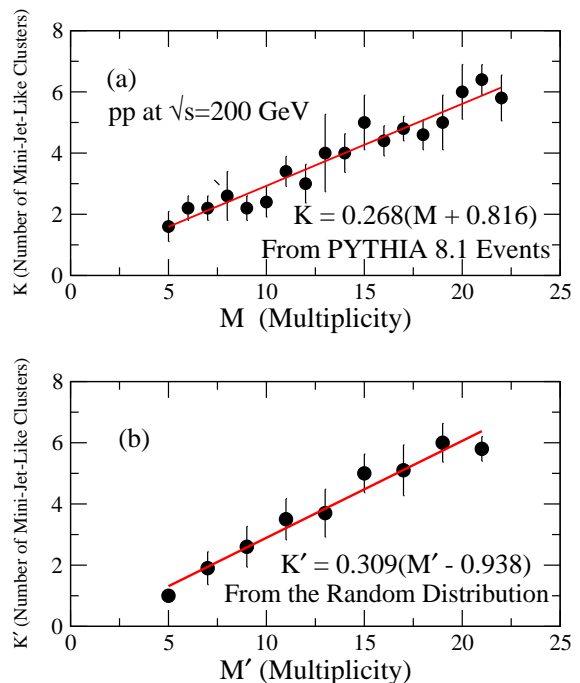


FIG. 7. (Color Online) Relations between charge multiplicity and the number of mini-jet-like clusters: (a) for pp collisions at $\sqrt{s} = 200$ GeV as extracted from events generated by PYTHIA 8.1 in Figs. 4-6, (b) for randomly distributed particles within $|\eta| \leq 1$ and $|\phi| \leq \pi$.

and $\{M', K'\}$ to emphasize that they are different sources of particle production that are likely to be collision-energy and detector-noise dependent.

We find in this case of random distribution that particle clustering also occurs when a large M' number of particles are produced randomly over a small phase space. To understand such a clustering, we can pick any two produced particles. The probability that a pair of particles falling randomly within the circle of radius R with respect to each other is

$$P_{\text{random}} = \left(\frac{\pi R^2}{2\pi \Delta\eta_{\text{window}}} \right). \quad (9)$$

In an event with multiplicity M' , the number of distinct pairs is

$$(\text{number of distinct pairs}) = \frac{M'(M' - 1)}{2}. \quad (10)$$

Therefore, in an event with multiplicity M' , the (average) number of clusters for the random distribution, $K'(2, M')$, is the product of Eqs. (9) and (10),

$$K'(2, M') = \frac{M'(M' - 1)}{2} \left(\frac{\pi R^2}{2\pi \Delta\eta_{\text{window}}} \right), \quad (11)$$

upon identifying a cluster as two particles falling within a radius of $R = 0.6$. However, because clusters can be formed with more than two particles, the above quantity $K'(2, M')$ represents therefore only the upper limit of the number of clusters when particles fall into and join other clusters.

More generally, the number $K'(n, M')$ of clusters of random coincidence for a cluster of n particles within a radius of R in an event with multiplicity M is

$$K'(n, M') = C_n^{M'} \left(\frac{\pi R^2}{2\pi \Delta\eta_{\text{window}}} \right)^{n-1}. \quad (12)$$

For the a detector with $\Delta\eta_{\text{window}}=2$ such as the STAR detector, we have

$$K'(2, M') = \frac{M'(M' - 1)}{2} \times 0.09. \quad (13)$$

Thus, the upper limit of the number of clusters from the random distribution Eq. (8) increases quadratically as a function of the multiplicity M' . This upper limit can be quite large for large M' . For example, one expects the upper limit of $K'(2, M') = 0.9$ and 4.95 clusters for $M'=5$ and $M'=11$ respectively. Thus, we would not be surprised to find clusters even for randomly and independently distributed particles as the multiplicity M' increases.

In our numerical example, we generate particles randomly with the uniform probability distribution of Eq. (8) within $-\pi \leq \phi \leq \pi$ and $-1 \leq \eta \leq 1$. We label the events as $xM'eI$ and show sample events with multiplicity $M'=5$ to $M'=21$ in Figs. 8 to 10, where we shall not distinguish the charges and the types of particles. We then use the mini-jet finding algorithm of Sections III

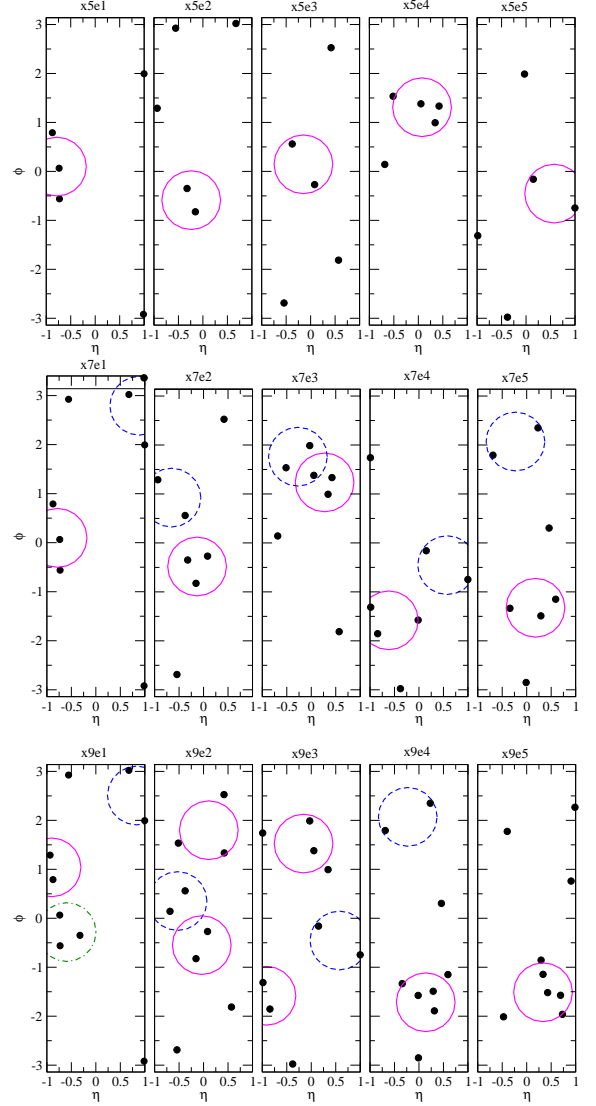


FIG. 8. (Color Online) Scatter plots in the (η, ϕ) plane for produced particles in events with multiplicities $M'=5, 7$, and 9, production within $|\eta| \leq 1$ and $|\phi| \leq \pi$. Circular curves indicate the locations of the cluster circles with $R = 0.6$.

and IV to locate mini-jet-like cluster centers and circumscribe the mini-jet-like cluster in circles, with approximately back-to-back clusters in circles of the same type. The average number of clusters is $\langle K' \rangle = 0.8$ for $M'=5$ in Fig. 8, and is $\langle K' \rangle = 3.2$ for $M'=11$ in Fig. 9, which approximately agree with the general trend on the increase in the upper limit of the number of clusters for randomly distributed events as $K'_{\text{random}} \leq 0.9$ for $M'=5$, and $K'_{\text{random}} \leq 4.95$ for $M'=11$, estimated from Eq. (13).

Figs. 8 to 10 show that as the multiplicity increases, the number of clusters K' also increases. In Fig. 7(b), we shows that for events generated by the random distribution in the phase space of $|\eta| \leq 1$ and $|\phi| \leq \pi$, the number of mini-jet-like clusters K' appears to be a linear

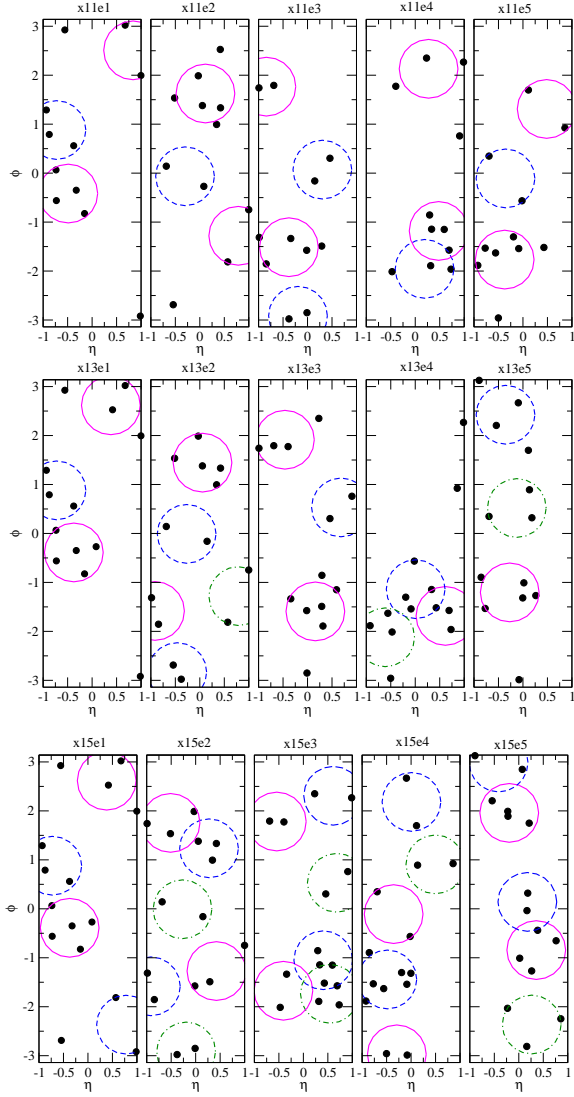


FIG. 9. (Color Online) Scatter plots in the (η, ϕ) plane for produced particles in events with multiplicities $M'=11, 13$, and 15 generated by an event generator with a uniform and independent production within $|\eta| \leq 1$ and $|\phi| \leq \pi$. Circular curves indicate the locations of the cluster circles with $R = 0.6$.

function of charge multiplicity M' given by

$$K' = (0.309 \pm 0.030)[M' - (0.938 \pm 1.304)], \quad (14)$$

which is similar to the dependence of the cluster number K and the multiplicity number M for events generated by PYTHIA8.1 in Eq. (7). We note that the number of clusters K' estimated by Eq. (11) represents only an upper limit, because a cluster with more than two particles can be formed in high multiplicity events. The number of clusters increases only linearly with multiplicity M' , instead of the quadratic dependence of Eq. (11), as shown in Fig. 7(b).

One way to study the clusters that are formed is by way of the $(\Delta\eta = \eta_1 - \eta_2, \Delta\phi = \phi_1 - \phi_2)$ correlations

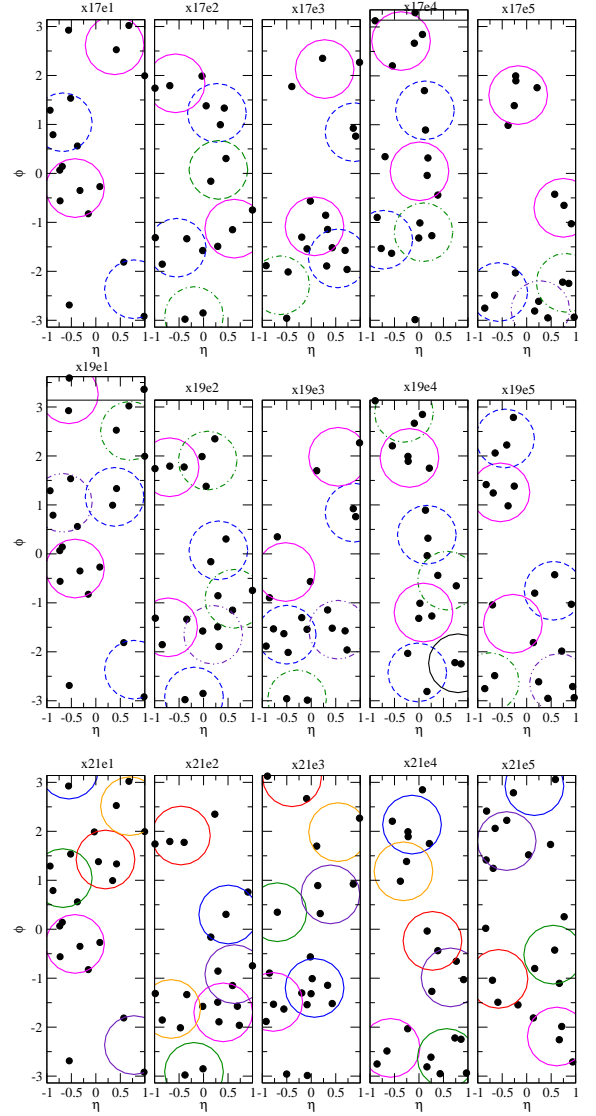


FIG. 10. (Color Online) Scatter plots in the (η, ϕ) plane for produced particles in events with multiplicities $M'=17, 19$, and 21 generated an event generator with a uniform and independent production within $|\eta| \leq 1$ and $|\phi| \leq \pi$. Circular curves indicate the locations of the cluster circles with $R = 0.6$.

between clusters located at (η_1, ϕ_1) and (η_2, ϕ_2) . Figs. 8 to 10 for the random and uniformly distributed particles also exhibit azimuthal corrections for some of the pairs, as cluster circles of similar types in these figures indicate. Thus, the clusters in the random distribution also exhibit approximate azimuthal back-to-back correlations, as can be observed in Figs. 9 and 10.

We can estimate the number of azimuthally back-to-back correlated mini-jet-like clusters D' as a function of the number of clusters K' . We consider a pair of mini-jet-like clusters. The probability that the pair of mini-jet-like clusters can be considered back-to-back correlated in

azimuthal angles is

$$P_{\text{random}} = \frac{2R}{2\pi}. \quad (15)$$

In an event with K' number of mini-jet-like clusters, the number of distinct mini-jet-like pairs is

$$(\text{number of distinct pairs}) = \frac{K'(K' - 1)}{2}. \quad (16)$$

Therefore, in such an event with K' number of mini-jet-like clusters, the (average) number of mini-dijet-like pairs $D'(K')$ for the random distribution, is the product of Eqs. (15) and (16),

$$D'(K') = \frac{K'(K' - 1)}{2} \left(\frac{R}{\pi} \right). \quad (17)$$

Thus, the number of mini-dijet-like pair is $D'(K')=1.15$ for $K'=4$. This means that when K' exceeds about 4 the number of mini-dijet-like pair of clusters $D' \sim 1$ and back-to-back correlated mini-dijet-like pair will begin to set in, as one can observe from the number of mini-dijet-like clusters in events x11e3, x13e2, and x15e1 with $K' \gtrsim 4$ in Fig. 9.

Results in Figs. 8 to 10 indicate that by distributing particles densely within a small angular phase space, clustering and azimuthal correlations occur also for randomly distributed source of particle. Thus, clustering and azimuthal correlation by themselves cannot be the only means of identifying mini-jets and mini-dijets. The identification of these clusters as such arises from other independent supports for the dominance of the hard-scattering model for mini-jet production of low- p_T particles.

VII. CONCLUSIONS AND DISCUSSIONS

The parton-parton hard scattering is an important process in high-energy nucleon-nucleon collisions. Although originally conceived to involve only the production of high- p_T particles, it has been suggested that the dominance of the hard-scattering process may extend to the low- p_T region, with the production of mini-jets and mini-dijets, as the collision energy increases.

As a first attempt to identify mini-jet and mini-dijets, we develop an algorithm to search for mini-jet-like clusters using the k-means clustering method, supplemented with a k-number (cluster-number) selection principle. The method adopts a scheme of random initialization of the initial centers, minimizing the potential function $\Phi(K)$ for a fixed K , and looking for the K number of clusters that leaves the fewest particles outside the cluster circles. The method is stable, fast, accurate, and yields mini-jet-like clusters and their associated particles.

Using such a method, we have located mini-jet-like clusters in the (η, ϕ) plane on an event-by-event basis, using events generated by PYTHIA8.1, which contains the

dynamics of multiple parton interactions. To a mini-jet-like cluster identified by the procedures, one often find an associated mini-jet-like cluster located at approximately $|\Delta\phi_{\text{jet-jet}}| \sim \pi \pm R$. Their azimuthal angular correlation suggests that they may be identified as the two partners of a mini-dijet-like pair. We find that mini-jet-like clusters, mini-dijet-like pairs, and multiple mini-dijet-like pairs of low- p_T hadrons are common occurrences for PYTHIA8.1 events with high multiplicities. The number of multiple mini-jet-like clusters and mini-dijet-like pairs increases with increasing multiplicity M .

It must be pointed out however that clustering and azimuthal correlations alone cannot be the only means to identify mini-jet and mini-dijets. A randomly distributed set of particles in large multiplicities also exhibit clustering properties similar to those from the PYTHIA8.1 program with mini-jets. The ability to separate out the mini-jet of multiplicity M from other sources of particles of multiplicity M' will depend on the ratio M/M' , which is likely to be collision-energy and detector-noise dependent. In this regard, the quantitative assessment of the dominance of the relativistic hard-scattering process in the low- p_T region needs to be independently established in order to identify the mini-jet-like clusters as physical mini-jets. The success of such an identification will provide a tool to investigate mini-jet and mini-dijet properties, for which not too much detail information has been collected. Furthermore, quantitative predictions based on first principles of perturbative QCD for the low- p_T region is difficult because the multiple collision probability involves higher-order corrections beyond the leading order [72]. Other possible non-perturbative QCD effects may also be present. The present investigation seeking ways to identify the multiple hard-scattering process may pave the way to a future semi-empirical phenomenological description of the multiple scattering process, with information obtained by direct mini-jet and mini-dijet analysis of the angular scatter plot of experimental event-by-event data.

From our investigations, one may also wish to develop parallel strategies to study mini-jets and mini-dijets. One way is to apply the proposed algorithm to examine experimental data at various energies and consider tentatively the mini-jet-like clusters to be physical mini-jets and study quantitative information on the production cross sections and the phase-space distribution of these objects, for comparison with the theory of multiple mini-jet production as a function of the collision energies. In this regard, we should note that the higher the pp collision energy, the greater is the probability of the dominance of the hard-scattering process for the production of low- p_T particles, and the greater will be the probability of the mini-jet-like clusters to be indeed physical mini-jets. It will be of interest is to see whether even higher multiple collisions of partons with a greater number of mini-dijets may lead to a black-disk type behavior as the path-length of the parton traversing through the target proton increases.

On a parallel track, one may like to lower the noise multiplicity M' by increasing the value of the lower bound of p_T , as mini-jets and harder jets becomes more and more dominant as the value of p_T increase. This will reduce the multiplicity of the noise or non-mini-jet particles. Alternatively, one can also consider only mini-jet clusters with a large number of particles. The increase in the number of particles in each cluster cuts down on the number of noise clusters and lower the noise in the identification of the mini-jets.

Acknowledgments

The authors would like to thank Profs. Zhenyu Ye and Soren Sorensen for helpful discussions. The research was supported in part by the Division of Nuclear Physics, U.S. Department of Energy under Contract DE-AC05-00OR22725 with UT-Battelle and Contract DE-FG02-88ER40424 with UCLA.

Appendix A: The “Elbow” Method of Cluster Number Selection

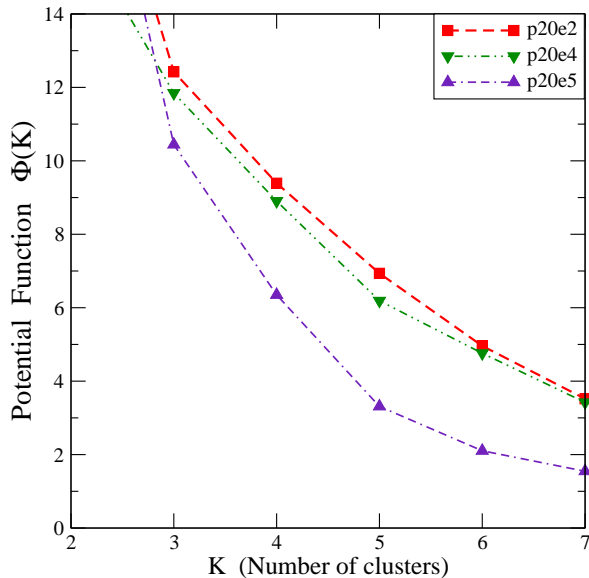


FIG. 11. (Color Online) The potential function $\Phi(K)$, the sum of square distances between the subset data points and their corresponding cluster centers, as a function of the number of clusters K , for minimum-bias events with multiplicity $M = 20$ generated by PYTHIA8.1.

There is another method to select the cluster number K by studying the K -dependence of the potential function $\Phi(K)$. For a given K value, after the minimization of the potential function $\Phi(K)$ with respect to the random initialization of the cluster centers and the variations of the cluster center positions, the quantity $\Phi(K)$ of Eq. (3) is then evaluated. The potential function $\Phi(K)$ is on the whole a decreasing function of increasing K (Fig. 11), as it reaches the limiting value of zero when the number of clusters K is the same as the number of data points M . An inefficient and slow decrease of $\Phi(K)$ occurs, if a cluster is subdivided into smaller sub-clusters with a subsequently smaller change of the $\Phi(K)$ slope. On the other hand, a large and abrupt change of $\Phi(K)$ as a function of K signifies a significant change of the structure of the clustering configuration and may be the location of the appropriate cluster number. Hence, it has been suggested that the proper cluster number K occurs at the kink (or ‘elbow’) of the curve of $\Phi(K)$ as a function of K or at the location of an abrupt change of the slope of $\Phi(K)$ [85, 90].

We calculate the potential function $\Phi(K)$ as a function of the cluster number K for events with $M = 20$ as shown in Fig. 2. For event p20e2 shown in Fig. 4, a kink of $P(K)$ occurs at $K=3$ and a very weak kink also appears to occur at $K=6$. The determination of the location of the “kink” is not without ambiguity. The elbow method would suggest the cluster number of $K=3$ or 6 but as we observed in Fig. 2, the proper cluster number as determined from the principle of fewest outside points is $K=7$. For event p20e4, kinks of $\Phi(K)$ occur at $K=3$ and 5, but the appropriate cluster number as determined from the principle of fewest outside points is 7. For p20e5, the potential function shows a sharp kink at $K=3$, and weaker kinks at 5, and 6 whereas the method of the principle of fewest outside points gives $K=6$. The method of the sharpest kink has the difficulty of recognizing the location of the kink, as many changes of slopes occur at different locations. If one takes the method to be given by the location with the greatest change of the magnitude of the slope, it would give K numbers which differ from the k-number selection principle of the fewest number of outside points.

We conclude that in the elbow method the determination on the location of the “kink” is ambiguous and there is no obvious method to resolve the ambiguities. The principle of the fewest outside points should be the proper criterion for the selection of the proper cluster number K as it is based on the physical property of the clustering of a mini-jet.

[1] R. Blankenbecler and S. J. Brodsky, Phys. Rev. D **10**, 2973 (1974); R. Blankenbecler, S. J. Brodsky and J. Gunion, Phys. Rev. D **12**, 3469 (1975); E. A. Schmidt and R. Blankenbecler, Phys. Rev. D **15**, 3321 (1977), R. Blankenbecler, A. Capella, J. Tran Thanh Van, C. Pa-

jares and A.V. Ramallo, Phys. Lett. **107B**, 106 (1981).
 [2] A.L.S. Angelis *et al.* (CCOR Collaboration), Phys. Lett. B **79**, 505 (1978).
 [3] R. P. Feynman, R. D. Field and G. C. Fox, Phys. Rev. D **18**, 3320 (1978).

- [4] J. F. Owens, E. Reya, and M. Glück, Phys. Rev. D **18**, 1501 (1978); D. W. Duke, J. F. Owens, Phys. Rev. D **30**, 49 (1984).
- [5] J. Rak and M. J. Tannenbaum, *High-pr Physics in the Heavy Ion Era*, Cambridge University Press, Cambridge, 2013.
- [6] T. Sjöstrand, Comp. Phys. Comm. **39**, 347 (1986); T. Sjöstrand and M. Bengtsson, Comp. Phys. Comm. **43**, 367 (1987).
- [7] T. Sjöstrand and M. van Zijl, Phys. Rev. **D36**, 2019 (1987).
- [8] T. Sjöstrand, S. Mrenna, P. Skands, *PYTHIA 6.4 Physics and Manual* JHEP **0605**, 026 (2006) [arXiv:hep-ph/0603175].
- [9] T. Sjöstrand, S. Mrenna, P. Skands, *A Brief Introduction to PYTHIA 8.1*, Comp. Phys. Comm. **178**, 852 (2008) [arXiv:0710.3820].
- [10] T. Sjöstrand *et al.*, *An Introduction to PYTHIA 8.2*, arXiv:1410.3012.
- [11] T. Sjöstrand and P. Z. Skands, JHEP **0403**, 053 (2005) [arxiv:hep-ph/040278].
- [12] T. Sjöstrand and P. Z. Skands, JHEP **0503**, 053 (2005) [arxiv:hep-ph/0408302].
- [13] R. Corke and T. Sjöstrand, JHEP **1103**, 032 (2011) [arXiv:1011.1759].
- [14] R. Corke and T. Sjöstrand, JHEP **1001**, 035 (2010) [arXiv:0911.1909].
- [15] C. Albajar *et al.* (UA1 Collaboration), Nucl. Phys. **B309**, 405 (1988).
- [16] K. S. Eskola, K. Kajantie, J. Lindfors, Nucl. Phys. **B323**, 37 (1989).
- [17] X.N. Wang and M. Gyulassy, Phys. Rev. **D44**, 3501.
- [18] G. Calucci and D. Treleani, Phys. Rev. **D41**, 3367 (1990).
- [19] G. Calucci and D. Treleani, Phys. Rev. **D44**, 2746 (1990).
- [20] G. Calucci and D. Treleani, Int. Jour. Mod. Phys. **A6**, 4375 (1991).
- [21] G. Calucci and D. Treleani, Phys. Rev. **D49**, 138 (1994).
- [22] G. Calucci and D. Treleani, Phys. Rev. **D50**, 4703 (1994).
- [23] G. Calucci and D. Treleani, Phys. Rev. **D63**, 116002 (2001).
- [24] A. Accardi and D. Treleani, Phys. Rev. **D64**, 116004 (2001).
- [25] C. Y. Wong, *Introduction to High-Energy Heavy-Ion Collisions*, World Scientific Publisher, 1994.
- [26] C.Y. Wong, G. Wilk, Acta Physica Polonica **B42**, 2047 (2012).
- [27] C.Y. Wong, G. Wilk, Phys. Rev. **D87**, 114007 (2013).
- [28] C.Y. Wong, G. Wilk, L.J.L. Cirto, C.Tsallis, EPJ Web Conf. **90**, 04002 (2015).
- [29] C.Y. Wong, G. Wilk, L.J.L. Cirto, C.Tsallis, Phys. Rev. **D91**, 114027 (2015).
- [30] Y. Nambu, Lectures at Copenhagen Symposium (1970).
- [31] J. D. Bjorken, Lectures presented at the 1973 Proceedings of the Summer Institute on Particle Physics, edited by Zipt, SLAC-167 (1973).
- [32] A. Casher, J. Kogut, and L. Susskind, Phys. Rev. **D10**, 732 (1974); A. Casher, H. Neuberger, and S. Nussinov, Phys. Rev. **D20** 179 (1979); Phys. Rev. **D21** 1966 (1980).
- [33] J. Schwinger, Phys. Rev. **128**, 2425 (1962); J. Schwinger, in *Theoretical Physics*, Trieste Lectures, 1962 (I.A.E.A., Vienna, 1963), p. 89.
- [34] X. Artru and G. Mennessier, Nucl. Phys. **B70**, 93 (1974).
- [35] B. Andersson, G. Gustafson and C. Peterson, Z. Phys. **C1**, 105 (1979); B. Andersson, G. Gustafson and B. Söderberg, Z. Phys. **C20**, 317 (1983).
- [36] A comprehensive review of the application of the Flux Tube Fragmentation Model for nucleon-nucleon and e^+e^- collisions can be found in B. Andersson, G. Gustafson, G. Ingelman, and T. Sjöstrand, Phys. Rep. **97**, 31 (1983), and X. Artru, Phys. Rep. **97**, 147 (1983).
- [37] X. Artru, Z. Phys. **C26**, 83 (1984).
- [38] B. Andersson, G. Gustafson, and T. Sjöstrand, Zeit. für Phys. **C20**, 317 (1983); T. Sjöstrand and M. Bengtsson, Computer Physics Comm. **43**, 367 (1987); B. Andersson, G. Gustafson, and B. Nilsson-Alqvist, Nucl. Phys. **B281**, 289 (1987).
- [39] J. Schwinger, Phys. Rev. **82**, 664 (1951).
- [40] R. C. Wang and C. Y. Wong, Phys. Rev. **D38**, 2890 (1988).
- [41] H-P. Pavel and D. Brink, Zeit. Phys. **C51**, 119 (1991).
- [42] C. Y. Wong, R. C. Wang, and C. C. Shih, Phys. Rev. **D44**, 257 (1991).
- [43] C. Y. Wong, R. C. Wang, Phys. Rev. **D44**, 679 (1991).
- [44] G. Gattoff and C.Y. Wong, Phys. Rev. **D 46**, 997 (1992); and C. Y. Wong and G. Gattoff, Phys. Rep. **242**, 1994, 489 (1994).
- [45] C. Y. Wong, R. C Wang, and J. S. Wu, Phys. Rev **D51**, 3940 (1995).
- [46] D.A. Derkach, G.A. Feofilov, Phys. Atom. Nucl. **71**, 2087 (2008); E.O. Bodnya, V.N. Kovalenko, A.M. Puchkov, G.A. Feofilov, AIP Conf.Proc. 1606, 273 (2014); Adam, Jaroslav *et al.*) JHEP 1505 (2015); G. Feofilov, I. Altsy-beev, O. Kochebina, XXII International Baldin Seminar on High Energy Physics Problems 15-20 September, 2014 JINR, Dubna, Russia, PoS(Baldin ISHEPP XXII) 067.
- [47] L. McLerran and R. Venugopalan, Phys. Rev. **D50**, 2225 (1994); J. Jalilian-Marian, A. Kovner, L. McLerran and H. Weigert, Phys. Rev. **D55**, 5414 (1997).
- [48] L. McLerran, "The Color Glass Condensate and Small x Physics: 4 Lectures", Lect.Notes Phys. **583**, 291, 2002, (arxiv:hep-ph/0104285).
- [49] L. McLerran, "The CGC and the Glasma: Two Lectures at the Yukawa Insitute", Prog. Theor. Phys. Suppl. **187**, 17 (2011), arXiv:1011.3204.
- [50] L. McLerran, "Strongly Interacting Matter Matter at Very High Energy Density: 3 Lectures in Zakopane", Acta Phys. Polon. **B41**, 2799 (2010), arXiv:1011.3203.
- [51] A. Kovner, L. McLerran, and H. Weigert, Phys. Rev. **D52**, 3809 (1995); A. Kovner, L. McLerran, and H. Weigert, Phys. Rev. **D52**, 6231 (1995).
- [52] F. Gelis, T. Lappi, and L. McLerran, Nucl. Phys. **A828**, 149 (2009); K. Fukushima, F. Gelis, and T. Lappi, Nucl. Phys. **A831**, 184 (2009); F. Gelis and N. Tanji, arXiv:1510.05454.
- [53] C. Y. Wong and R. Blankenbecler, Phys. Rev. **D22**, 2433 (1978)
- [54] The hard-scattering jet-production invariant cross section at mid-rapidity varies approximately as $\alpha_s^2 \sqrt{s}/p_T/p_T^4$, as a function of the pp collision energy \sqrt{s} and the jet p_T at high collision energies, (see for example the analytical expression of Eq. (14) of [29], obtained by integrating approximate parton structure functions).
- [55] J. Adams *et al.*, for the STAR Collaboration, Phys. Rev. Lett. **95**, 152301 (2005).
- [56] J. Adams *et al.* (STAR Collaboration), Phys. Rev. C **74**, 032006 (2006).
- [57] R. J. Porter and T. A. Trainor, (STAR Collaboration),

- J. Phys. Conf. Ser. **27**, 98 (2005).
- [58] T. A. Trainor and R. L. Ray, Phys. Rev. C **84**, 034906 (2011).
- [59] J. Adams *et al.* for the STAR Collaboration, Phys. Rev. Lett. **95**, 152301 (2005).
- [60] J. Adams *et al.* (STAR Collaboration), Phys. Rev. **C73**, 064907 (2006).
- [61] J. Putschke (STAR Collaboration), J. Phys. **G74**, S679 (2007).
- [62] J. Bielcikova (STAR Collaboration), J. Phys. **G74**, S929 (2007).
- [63] F. Wang (STAR Collaboration), Invited talk at the XIth International Workshop on Correlation and Fluctuation in Multiparticle Production, Hangzhou, China, November 2007, [arXiv:0707.0815].
- [64] C. Y. Wong, Phys. Rev. **C76**, 054908 (2007).
- [65] C. Y. Wong, Phys. Rev. **C78**, 064905 (2008).
- [66] C. Y. Wong, Phys. Rev. **C80**, 034908 (2009).
- [67] A. Adare, *et al.* (PHENIX Collaboration), Phys. Rev. C **78**, 014901 (2008); Phys. Rev. D **83**, 052004 (2011) and Phys. Rev. C **83**, 064903 (2011).
- [68] T. Akesson *et al.* (Axial Field Spectrometer Collaboration), Z. Phys. C **34**, 163 (1987).
- [69] F. Abe *et al.* (CDF Collaboration), Phys. Rev. Lett. **79**, 584 (1997). F. Abe *et al.* (CDF Collaboration), Phys. Rev. D **56**, 3811 (1997).
- [70] V. M. Abazov *et al.* (D0 Collaboration), Phys. Rev. D **81**, 052012 (2010).
- [71] S. Chatrchyan *et al.*, (CMS Collaboration), Phys. Rev. D **89**, 092010 (2014).
- [72] P. Kotko, A. M. Stasto, and M. Strikman, Phys. Rev. D **95**, 054009 (2017).
- [73] V. Khachatryan *et al.* (CMS Collaboration), J. High Energy Phys. **09**, 091 (2010) [arXiv:1009.4122]; CMS Collaboration, arXiv:1105.2438 (2011);
- [74] V. Khachatryan *et al.* (CMS Collaboration), *Measurement of Long-Range Near-Side Two-Particle Angular Correlations in pp Collisions at $s=13\text{TeV}$* , Phys. Rev. Lett. **116** (2016) 172302 [arXiv:1510.03068].
- [75] V. Khachatryan *et al.* (CMS Collaboration), *Evidence for collectivity in pp collisions at the LHC*, [arXiv:1606.06198].
- [76] A. Milov (ATLAS Collaboration), *Measurement of long-range particle correlations in small systems with the ATLAS detector*, arXiv:1612.08164.
- [77] K. Burka (ATLAS Collaboration), *Measurement of the ridge correlations in pp and pPb collisions with the ATLAS detector at the LHC*, PoS DIS2016 (2016) 053.
- [78] V. Zaccaro (ALICE Collaboration), *Charged-Particle Multiplicity Distributions over Wide Pseudorapidity Range in Proton-Proton and Proton-Lead Collisions with ALICE*, CERN-THESIS-2015-364.
- [79] E. Pereira De Oliveira Filho (ALICE Collaboration), *Study of the angular correlation between heavy-flavour decay electrons and charged unidentified particles in pp and p-Pb collisions with ALICE*, CERN-THESIS-2014-373.
- [80] C. Y. Wong, Phys. Rev. **C84**, 024901 (2011).
- [81] C. Y. Wong, *Event-by-Event Study of Space-Time Dynamics in Flux-Tube Fragmentation*, Jour. Phys. **G 44**, 075102 (2017) (arXiv:1510.07194).
- [82] D. M. Kaplan *et al.*, Phys. Rev. Lett. **40**, 435 (1978).
- [83] C. Y. Wong and H. Wang, Phys. Rev. **C58**, 376 (1998).
- [84] D. W. Duke and J. F. Owens, Phys. Rev. **D30**, 49 (1984); J. F. Owens, Rev. Mod. Phys. **59**, 465 (1987).
- [85] For an online introduction to k-means method, see Jack Ng, *Lectures in Machine Learning*, Stanford University, (2017): <https://www.coursera.org/learn/machine-learning/lecture/czmip/unsupervised-learning-introduction>.
- [86] H. Steinhaus, "Sur la division des corps matériels en parties", Bull. Acad. Polon. Sci. (in French). **4** (12): 801 (1957).
- [87] S. P. Lloyd, *Least squares quantization in pcm*, IEEE Transactions on Information Theory, **28**, 129 (1982).
- [88] MacQueen, J. B. "Some Methods for classification and Analysis of Multivariate Observations", Proceedings of 5th Berkeley Symposium on Mathematical Statistics and Probability. University of California Press. pp. 281297 (1967).
- [89] D. Arthur and S. Vassilvitskii, Proceedings of the eighteenth annual ACM-SIAM Symposium on Discrete algorithm, 1027 (2007).
- [90] R. L. Thorndike, Psychometrika **18** 267 (1953).
- [91] S. Chekanov, Eur. Phys. J. **C47**, 611 (2006).